Available online at www.sciencedirect.com
ScienceDirect
Thermochimica Acta 467 (2008) 91–98
thermochimica acta
www.elsevier.com/locate/tca

Thermal analysis of biodegradable microparticles containing ciprofloxacin hydrochloride obtained by spray drying technique

Arnóbio A. Silva-Júnior [a], Maria Virgínia Scarpa [a], Kelly Chrystina Pestana [a], Lucildes Pita Mercuri [b], Jivaldo Rosário de Matos [c], Anselmo Gomes de Oliveira [a,*]

[a] *Programa de Pós-graduação em Ciências Farmacêuticas, Faculdade de Ciências Farmacêuticas, Universidade Estadual Paulista-Unesp, Araraquara, SP, Brazil*
[b] *Centro de Ciências Exatas e Tecnologia, Cetec, Universidade Cruzeiro do Sul, São Paulo, SP, Brazil*
[c] *Departamento de Química Fundamental, Instituto de Química, Universidade de São Paulo, USP, São Paulo, SP, Brazil*

Received 18 June 2007; received in revised form 31 October 2007; accepted 31 October 2007

Abstract

Thermal analysis has been extensively used to obtain information about drug–polymer interactions and to perform pre-formulation studies of pharmaceutical dosage forms. In this work, biodegradable microparticles of poly(D,L-lactide-*co*-glycolide) (PLGA) containing ciprofloxacin hydrochloride (CP) in various drug:polymer ratios were obtained by spray drying. The main purpose of this study was to investigate the effect of the spray drying process on the drug–polymer interactions and on the stability of microparticles using differential scanning calorimetry (DSC), thermogravimetry (TG) and derivative thermogravimetry (DTG) and infrared spectroscopy (IR). The results showed that the high levels of encapsulation efficiency were dependant on drug:polymer ratio. DSC and TG/DTG analyses showed that for physical mixtures of the microparticles components the thermal profiles were different from those signals obtained with the pure substances. Thermal analysis data disclosed that physical interaction between CP and PLGA in high temperatures had occurred. The DSC and TG profiles for drug-loaded microparticles were very similar to the physical mixtures of components and it was possible to characterize the thermal properties of microparticles according to drug content. These data indicated that the spray dryer technique does not affect the physicochemical properties of the microparticles. In addition, the results are in agreement with IR data analysis demonstrating that no significant chemical interaction occurs between CP and PLGA in both physical mixtures and microparticles. In conclusion, we have found that the spray drying procedure used in this work can be a secure methodology to produce CP-loaded microparticles.

Keywords: Ciprofloxacin hydrochloride; Microparticles; Spray drying; Thermal analysis

1. Introduction

Ciprofloxacin hydrochloride (3-quinolinecarboxylic acid, 1-cyclopropyl-6-fluoro-1,4-dihydro-4-oxo-7-(1-piperazinyl)-, monohydrochloride, monohydrate) (CP) is a quinolone-carboxylic acid derivative with high antibiotic activity against gram-positive and gram-negative bacteria [1–3] (Fig. 1).

The development of a controlled release system for CP is very interesting for post-surgery prophylaxis, prevention and treatment of infections. Poly(D,L-lactide-*co*-glycolide) (PLGA) is a copolymer of lactic and glycolic acids widely used in drug release systems, due to its biocompatibility and biodegradation [4–7] (Fig. 2).

In recent years, many drug carrier systems containing biodegradable polymers such as nano- and microparticles have received attention, due to their ability to prolong the release, to target, and to protect drugs from degradation in the blood stream [8,9].

For obtaining the pharmacological effects of drugs with microparticles, it is necessary to establish, to characterize the drug–polymer interactions, and to determine the effect of the microencapsulating process on the physical and chemical stabilities of the components [10–12].

Thermal analysis is a very useful technique for evaluating a range of different samples of the same material, to assess the influence of excipients and microencapsulating process on the

* Corresponding author at: Departamento de Fármacos e Medicamentos, Faculdade de Ciências Farmacêuticas, Unesp, Rodovia Araraquara-Jaú km 01, 14801-902 Araraquara, SP, Brazil. Tel.: +55 16 33016974; fax: +55 16 33016960.
E-mail address: oliveiag@fcfar.unesp.br (A.G. de Oliveira).

0040-6031/$ – see front matter © 2007 Elsevier B.V. All rights reserved.
doi:10.1016/j.tca.2007.10.018

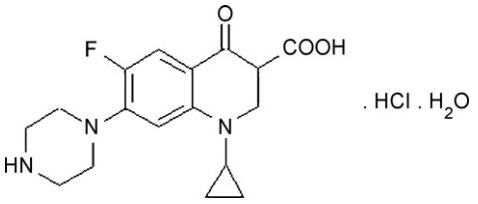

Fig. 1. Chemical structure of ciprofloxacin hydrochloride.

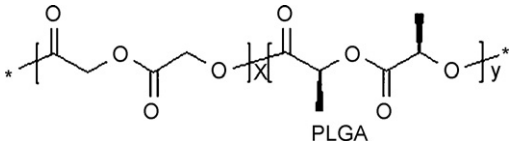

Fig. 2. Chemical structure of D,L-poly(lactide-*co*-glycolide) acid (PLGA).

physico-chemical properties of pharmaceutical materials and pharmaceutical dosage forms [13–18]. Moreover, DSC analysis can provide qualitative and quantitative information about the drug in the microparticles [19–26].

In this study, the spray drying process was used for the obtainment of the CP-loaded microparticles in various drug:polymer proportions. The effect of the process on the drug–polymer interactions was investigated by thermal analysis (DSC, TG and DTG) and infrared spectroscopy (IR). Physical mixtures with drug:polymer ratios identical to those used in the microparticles were used as control.

2. Experimental

2.1. Materials

Ciprofloxacin hydrochloride (CP) was purchased from Sigma–Aldrich Inc. (U.S.A.), PLGA 50:50 (inherent viscosity 0.63 dl/g at 30 °C) was purchased from Birmingham Polymer Inc. (U.S.A.), and ethanol and glacial acetic acid were from Merck S.A. (Brazil). Water was prepared with a Milli-Q Plus water purification system (Millipore) and its resistivity was 18.2 MΩ cm. All other solvents and chemicals were of analytical grade.

2.2. Microparticles preparation

Suitable amounts of CP were dissolved in ethanol–water (1:1, v/v) and added to polymer solutions in acetone to obtain mixtures with drug:polymer proportions of 1:1, 1:2, 1:3 and 1:5 (w/w). Microparticles were obtained by spraying the solutions through a mini spray dryer Büchi-191 equipped with a 0.7 mm nozzle at 206 kPa. The microparticles were collected and stored under vacuum at room temperature for 48 h.

2.3. Morphology and particle size analysis

The microparticles' shape and morphology were accessed with scanning electronic microscopy (SEM) and the particle size analysis was performed using an image processing software, Leika qwin® by Feret diameter method.

2.4. Drug encapsulation efficiency

Drug-loaded PLGA microparticles with theoretical CP content of 2 mg were dissolved in 10 ml of glacial acetic acid, and diluted in 0.1 M acetic acid to obtain a CP concentration of 10 μg ml^{-1}. The amount of the encapsulated drug was determined by UV–vis spectrophotometry at 278 nm. The drug concentration was determined from a standard curve obtained in 0.1 M acetic acid. The analytical method had previously been validated [27]. The analyses were performed in triplicate. The drug encapsulation efficiency was calculated from the ratio between the analytical and theoretical drug contents.

2.5. Thermal analysis

Differential scanning calorimetry (DSC) curves were carried out in a DSC-50 cell (Shimadzu) using aluminum pans with lids with about 1 mg of samples, under dynamic nitrogen atmosphere (100 ml min^{-1}), at a heating rate of 10 °C min^{-1}, and temperature range from 25 to 500 °C. The DSC cell was calibrated with Indium (melting point 156 °C and $\Delta H = 28.4$ J g^{-1}) and zinc standards (melting point 419.4 °C). Thermogravimetry (TG) and derivative thermogravimetry (DTG) curves were obtained from 5 mg samples with a thermobalance Shimadzu TGA-50, using platinum pans under dynamic nitrogen atmosphere (50 ml min^{-1}), at a heating rate of 10 °C min^{-1} and temperature range from 25 to 900 °C.

2.6. Infrared spectroscopy (IR)

IR was performed on the pure drug, pure polymer, drug-loaded microparticles and 1:1 (w/w) drug–polymer physical mixtures at ambient temperature, in the range of 400–4000 cm^{-1}, using KBr pellets in a Shimadzu FTIR-8300 spectrometer.

3. Results and discussions

The successfully produced CP-loaded PLGA using the specific parameters selected in the spray drying procedure was a white powder, visually uniform in size. The SEM confirmed this characteristic (Fig. 3). The images of Fig. 3 indicated mostly the spherical particle for all drug-loaded PLGA microparticles, which is an important technological property for powders, mainly due to the drug release rate from the polymeric matrix.

The mean diameter of the particles was assessed and the values identified were very similar to different microparticles. The results for particle size analysis and drug loading efficiency are shown in Table 1.

Good levels of drug loading were determined for all microparticle systems. According to the drug:polymer ratio, the drug-loading efficiencies were achieved in the range of 90.5–105.5%, demonstrating complete encapsulation of the CP in the microparticles. Using drug proportions similar to those measured in the microparticles, physical drug:polymer mixtures were used as control for thermal analysis studies.

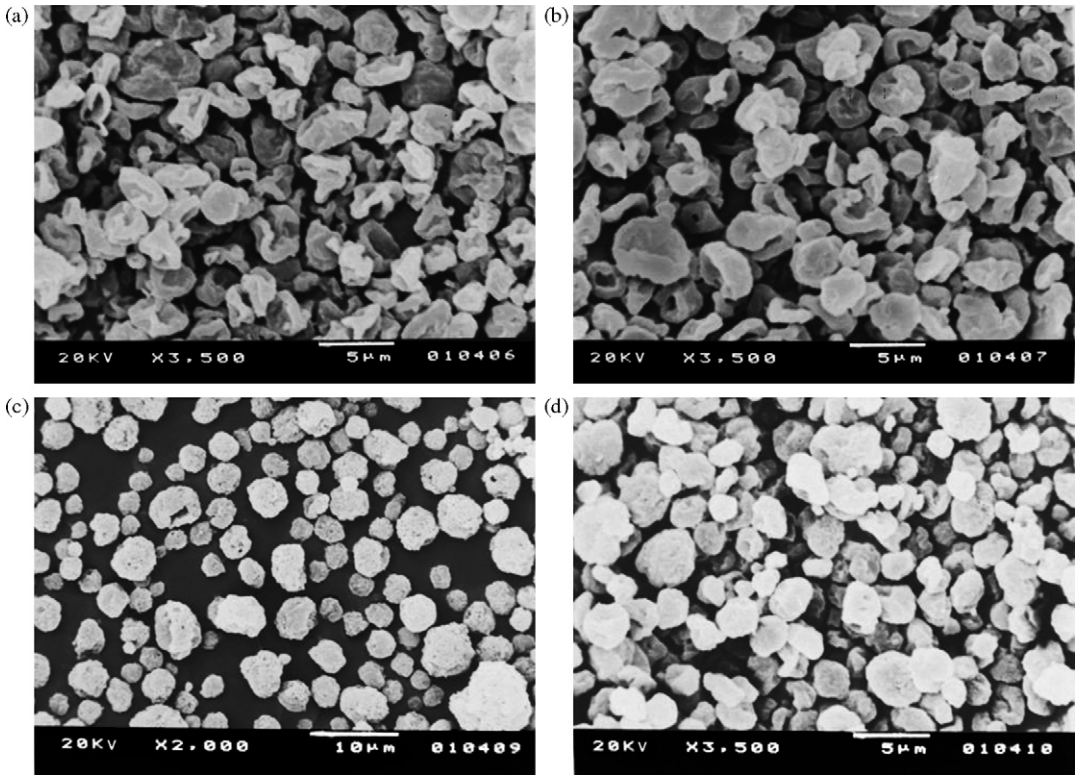

Fig. 3. SEM images of ciprofloxacin-loaded PLGA microparticles with drug/polymer proportions (w/w) of (a) 1:1; (b) 1:2; (c) 1:3; (d) 1:5.

Table 1
Rate of ciprofloxacin hydrochloride encapsulated into microparticles

Theoretical drug/polymer ratio	Mean diameter (μm)	Analytical drug content (%)	Rate of encapsulation
1:1	2.45 ± 0.80	49.93 ± 0.20	0.998 ± 0.008
1:2	2.60 ± 0.60	30.18 ± 1.54	0.905 ± 0.031
1:3	2.32 ± 0.54	24.51 ± 0.52	0.981 ± 0.009
1:5	3.09 ± 0.31	21.09 ± 0.67	1.055 ± 0.011

The DSC and TG/DTG curves for pure CP are shown in Fig. 4.

The DSC curve for CP shows a first endothermic peak in the range of 104–140 °C ($\Delta H = -133.18\,J\,g^{-1}$), due to sample dehydration, which was confirmed by a weight loss of 4.5% verified in the range of 113.4–139.8 °C in the TG/DTG curves. The exothermic event was in the range of 152.8–184 °C ($\Delta H = +29.3\,J\,g^{-1}$) is a characteristic of some disordered crystallization or amorphous drug phase [28]. A second endothermic event in the range of 285–315 °C ($\Delta H = -163.85$) may be attributed to the drug decomposition just after its melting. From TG/DTG curves could be observed that the second event of weight loss occurred only beyond 299.3 °C. These results of DSC and TG/DTG for CP are in agreement with the reported data in the literature [29,30].

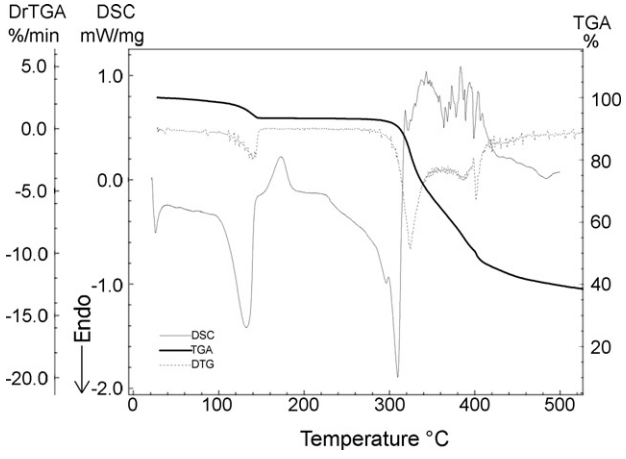

Fig. 4. DSC and TG/DTG curves for ciprofloxacin hydrochloride in a dynamic nitrogen atmosphere, respectively, at 100 and 50 ml min^{-1} at a heating rate of 10 °C min^{-1}.

The DSC curve and TG/DTG thermograms for pure PLGA are shown in Fig. 5.

From the DSC curve of PLGA is possible to observe two thermal events. The glass transition of polymer occurred in the range of 45.5–52.4 °C with an enthalpy of relaxation of 0.05 mW mg^{-1} and midpoint of 43.12 °C. The endothermic degradation of PLGA occurred on a single step in the range of 309.2–381.0 °C ($\Delta H = 550.6\,J\,g^{-1}$) with a weight loss of 90.1%.

The physical and chemical interactions between drug and polymer were studied with the aim of predicting the thermal behavior of the biodegradable microparticles. Thus, physical

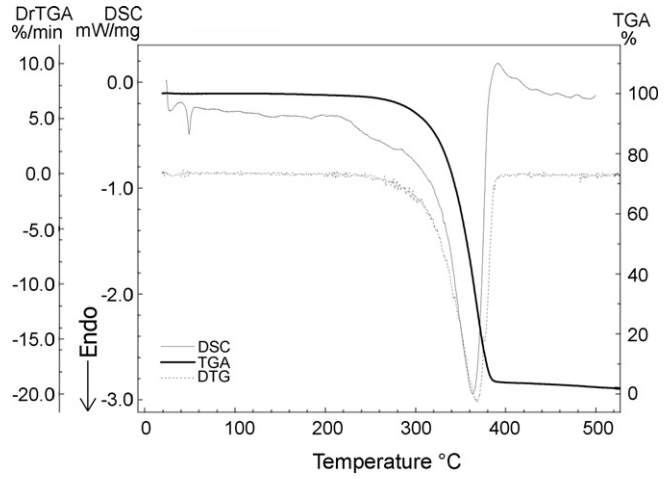

Fig. 5. DSC and TG/DTG curves of PLGA in a dynamic nitrogen atmosphere, respectively, at 100 and 50 ml min^{-1} at a heating rate of 10 °C min^{-1}.

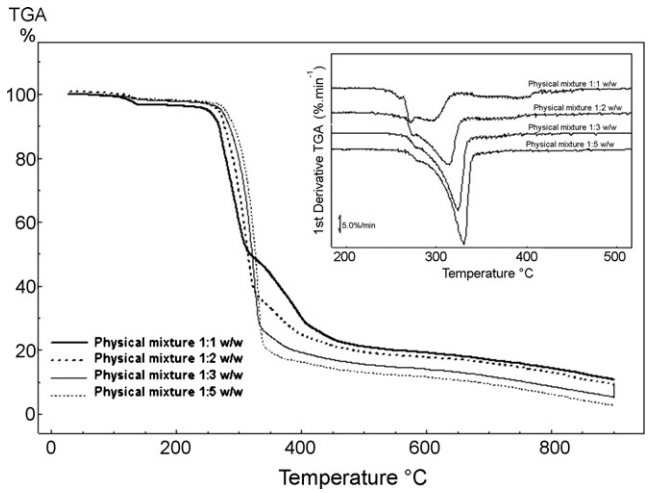

Fig. 7. TG and DTG curves for different physical mixtures at a heating rate of 10 °C min^{-1}.

mixtures of drug and polymer with identical proportions to the drug-loaded microparticles were analyzed by DSC and TG/DTG. In Fig. 6 are shown the DSC curves for different physical mixtures.

The glass transition of PLGA occurred in the range of 45–53 °C, followed by an endothermic event in the range of 99–140 °C, due to dehydration of drug present in the sample. The absence of the phase transition in the range of 152–184 °C (Fig. 4) may be due to the possible dissolution of drug fraction during the polymer melting while heating. This was well characterized when carriers with low melting point/glass transition were used [31–34], and consequently the appearance of the drug melting point at lower temperature than that occurred in the neat drug, with decomposition just a beginning of drug melting in the range of 220–280 °C. The endothermic decomposition of polymer occurred in the temperature range of 282–330 °C. The thermal events of weight loss were confirmed by TG/DTG data (Fig. 7), and it was possible to identify clearly three steps. The first occurred in the range of 100–140 °C due dehydration, the second in the range of 252–330 °C due decomposition of drug and the third in the range of 315–420 °C due decomposition of polymer. After these, the decomposition of material occurs slowly. The beginning and intensity of the thermal events varied according to drug:polymer proportion.

After characterizing the thermal properties of the physical mixtures, it was performed the DSC analysis of the different drug-loaded microparticles (Fig. 8). The glass transition of PLGA occurred in the range of 45–53 °C. An endothermic event due to dehydration occurred in range of 98–123 °C. The second endothermic event occurred in the range of 231–280 due to the beginning of decomposition during drug melting. A third endothermic event was observed in the temperature range of about 275–330 °C followed by exothermic events.

From TG/DTG data (Fig. 9) a first event of weight loss was identified in the range of 102–135 °C due to dehydration, the second in the range of 243–337 °C occurred due to drug decomposition and a third event in the range of 315–404 °C due to decomposition of polymer. After these, the decomposition of material occurred slowly. The beginning and intensity of the thermal events varied according to drug:polymer proportion.

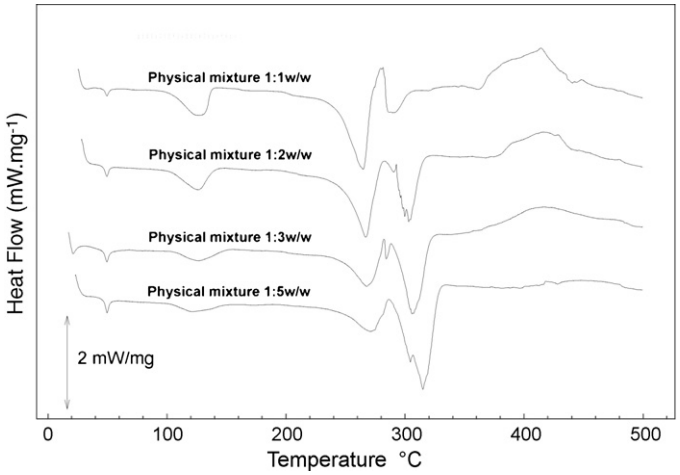

Fig. 6. DSC curves for the different physical mixtures at a heating rate of 10 °C min^{-1}.

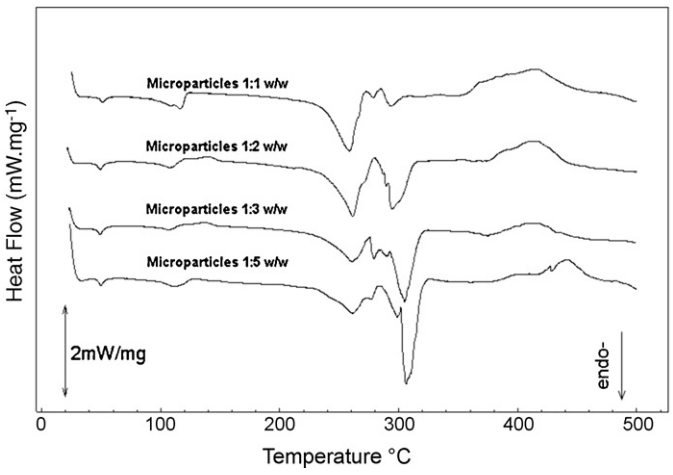

Fig. 8. DSC curves for different CP-loaded PLGA microparticles at a heating rate of 10 °C min^{-1}.

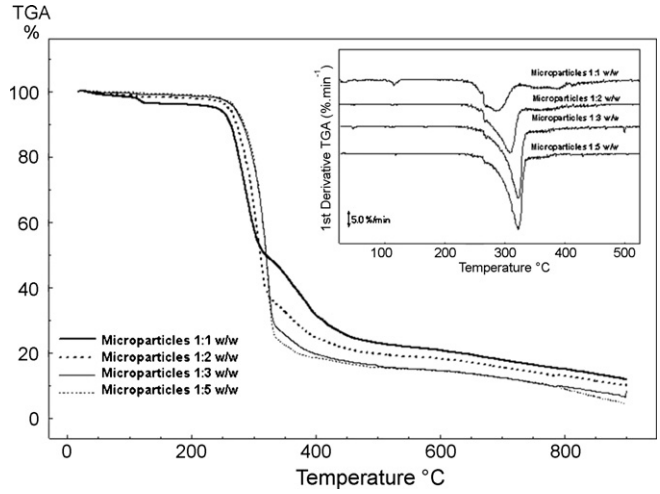

Fig. 9. TG curves for CP-loaded PLGA microparticles at a heating rate of 10 °C min^{-1}.

With the purpose to evaluate the effect of the spray drying microencapsulating process on the drug–polymer interactions and on the stability of microparticles, the data from thermal analysis of different drug-loaded PLGA microparticles (Mcs) was correlated with the respective physical mixtures (PMs) (Table 2). The temperature ranges of the thermal events were very similar, indicating that the experimental selected conditions for preparation of drug-loaded PLGA microparticles did not changed the components stability. However, the enthalpy values involved in the thermal events obtained for CP-loaded microparticles were different from those determined for the respective physical mixture. This could be attributed to different aggregation states of the drug present in different samples. It may be evidenced by a lower relaxation enthalpy identified for the glass transition of the polymer in the microparticles than those obtained for the physical mixtures. It is well established that the particles produced by spray drying technique have a different aggregation state from physical mixtures [35–38].

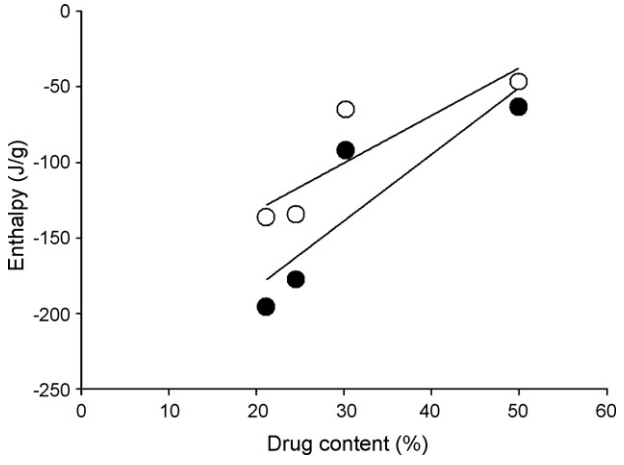

Fig. 10. Correlation of enthalpy values and drug content determined for drug decomposition just a beginning of melting drug. (●) physical mixtures, (○) CP-loaded PLGA microparticles.

Table 2
Thermal properties determined for drug–polymer physical mixtures (PMs) and drug-loaded microparticles (Mcs)

Sample	First event	Second event	Third event	Fourth event
DSC				
PM (1:1, w/w)	45.6–52.3 °C (43.3) [$\Delta H = -0.03$ mW mg^{-1}]	100–137 (125.9 °C) [$\Delta H = -62.1$ J g^{-1}]	220–273 (264.9 °C) [$\Delta H = -195.7$ J g^{-1}]	281–309 (289.6 °C) [$\Delta H = -66.4$ J g^{-1}]
PM (1:2, w/w)	46.1–52.8 (44.4 °C) [$\Delta H = -0.07$ mW mg^{-1}]	101–138 (125.9 °C) [$\Delta H = -44.4$ J g^{-1}]	225–279 (266.9 °C) [$\Delta H = -177.4$ J g^{-1}]	284–314 (303.2 °C) [$\Delta H = -96.9$ J g^{-1}]
PM (1:3, w/w)	46.6–52.3 (45.9 °C) [$\Delta H = -0.06$ mW mg^{-1}]	102–147(126.8 °C) [$\Delta H = -31.7$ J g^{-1}]	234–280 (267.9 °C) [$\Delta H = -91.9$ J g^{-1}]	282–319 (306.0 °C) [$\Delta H = -131.0$ J g^{-1}]
PM (1:5, w/w)	46.6–52.7 (45.2 °C) [$\Delta H = -0.08$ mW mg^{-1}]	104–146 (120.6 °C) [$\Delta H = -23.1$ J g^{-1}]	240–283 (270.8 °C) [$\Delta H = -63.3$ J g^{-1}]	287–330 (314.9 °C) [$\Delta H = -264.2$ J g^{-1}]
Mc (1:1, w/w)	45.7–52.7 (53.0 °C) [$\Delta H = -0.04$ mW mg^{-1}]	98–122 (116.5 °C) [$\Delta H = -20.4$ J g^{-1}]	233–270 (258.5 °C) [$\Delta H = -136.3$ J g^{-1}]	286–303 (293.6 °C) [$\Delta H = -17.50$ J g^{-1}]
Mc (1:2, w/w)	45.7–52.7 (52.9 °C) [$\Delta H = -0.04$ mW mg^{-1}]	98–118 (108.2 °C) [$\Delta H = -7.9$ J g^{-1}]	231–277 (261.3 °C) [$\Delta H = -134.3$ J g^{-1}]	282–311 (294.4 °C) [$\Delta H = -107.9$ J g^{-1}]
Mc (1:3, w/w)	45.7–52.7 (52.3 °C) [$\Delta H = -0.04$ mW mg^{-1}]	99–114 (106.8 °C) [$\Delta H = -3.8$ J g^{-1}]	231–274 (260.6 °C) [$\Delta H = -65.0$ J g^{-1}]	275–316 (305.0 °C) [$\Delta H = -166.3$ J g^{-1}]
Mc (1:5, w/w)	45.7–52.7 (52.3 °C) [$\Delta H = -0.04$ mW mg^{-1}]	99–123 (111.6 °C) [$\Delta H = -10.9$]	232–280 (261 °C) [$\Delta H = -46.72$ J g^{-1}]	286–319 (306.0 °C) [$\Delta H = -172$ J g^{-1}]
Sample	First event	Second event	Third event	
TGA				
PM (1:1, w/w)	108.3–137.4 [$T_{max} = 132$ °C ($\Delta m = 2.3\%$)]	251.8–315.2 [$T_{max} = 296$ °C ($\Delta m = 44.0\%$)]	315.2–420.8 [$T_{max} = 394$ °C ($\Delta m = 24.22\%$)]	
PM (1:2, w/w)	107.1–141.8 [$T_{max} = 124$ °C ($\Delta m = 1.8\%$)]	253.1–324.2 [$T_{max} = 315$ °C ($\Delta m = 57.7\%$)]	324.3–404.9 [$T_{max} = 366$ °C ($\Delta m = 14.67\%$)]	
PM (1:3, w/w)	109.8–146.5 [$T_{max} = 124$ °C ($\Delta m = 1.2\%$)]	260.2–333.13 [$T_{max} = 325$ °C ($\Delta m = 68.5\%$)]	333.1–389.4 [$T_{max} = 381$ °C ($\Delta m = 8.2\%$)]	
PM (1:5, w/w)	105.8–149.0 [$T_{max} = 131$ °C ($\Delta m = 1.5\%$)]	257.2–342.7 [$T_{max} = 331$ °C ($\Delta m = 76.5\%$)]	342.7–376.3 [$T_{max} = 348$ °C ($\Delta m = -3.6\%$)]	
Mc (1:1, w/w)	102.4–127.8 [$T_{max} = 117$ °C ($\Delta m = 1.8\%$)]	241.1–315.1 [$T_{max} = 287$ °C ($\Delta m = 44.4\%$)]	315.08–404.48 [$T_{max} = 391$ °C ($\Delta m = -20\%$)]	
Mc (1:2, w/w)	106.6–117.4 [$T_{max} = 115$ °C ($\Delta m = 0.3\%$)]	243.2–321.9 [$T_{max} = 310$ °C ($\Delta m = 57.9\%$)]	321.89–404.43 [$T_{max} = 365$ °C ($\Delta m = 14.7\%$)]	
Mc (1:3, w/w)	101.1–130.2 [$T_{max} = 123$ °C ($\Delta m = 0.3\%$)]	260.4–334.3 [$T_{max} = 323$ °C ($\Delta m = 67.9\%$)]	334.3–399.4 [$T_{max} = 359$ °C ($\Delta m = 8.8\%$)]	
Mc (1:5, w/w)	102.0–135.2 [$T_{max} = 120$ °C ($\Delta m = 0.4\%$)]	270.4–336.7 [$T_{max} = 324$ °C ($\Delta m = 70.4\%$)]	336.7–386.0 [$T_{max} = 342$ °C ($\Delta m = 5.6\%$)]	

The glass transition temperature (T_g) is an important parameter to characterize the mechanical behavior of glassy amorphous pharmaceuticals [39–41]. The molecular mobility of the polymeric chains has an important role in deciding the mechanical properties, diffusion of small molecules through the polymeric matrix, and the enthalpy involved in the thermal event may vary with the drug content into polymeric matrix [41]. However, it was not possible to establish a correlation between the drug loading of different microparticles and the relaxation enthalpy for glass transition. On the contrary, for other ther-

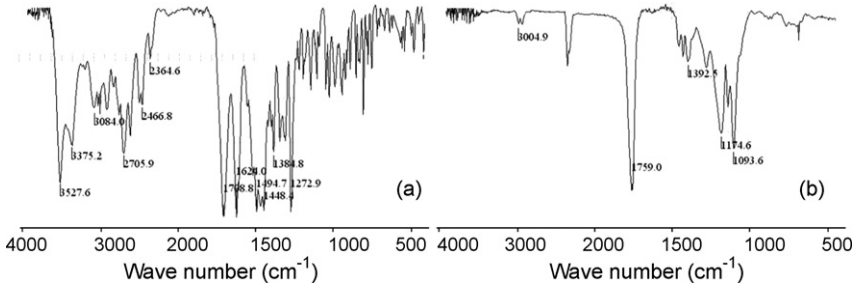

Fig. 11. The infrared spectra (IR) for both (a) ciprofloxacin and (b) PLGA.

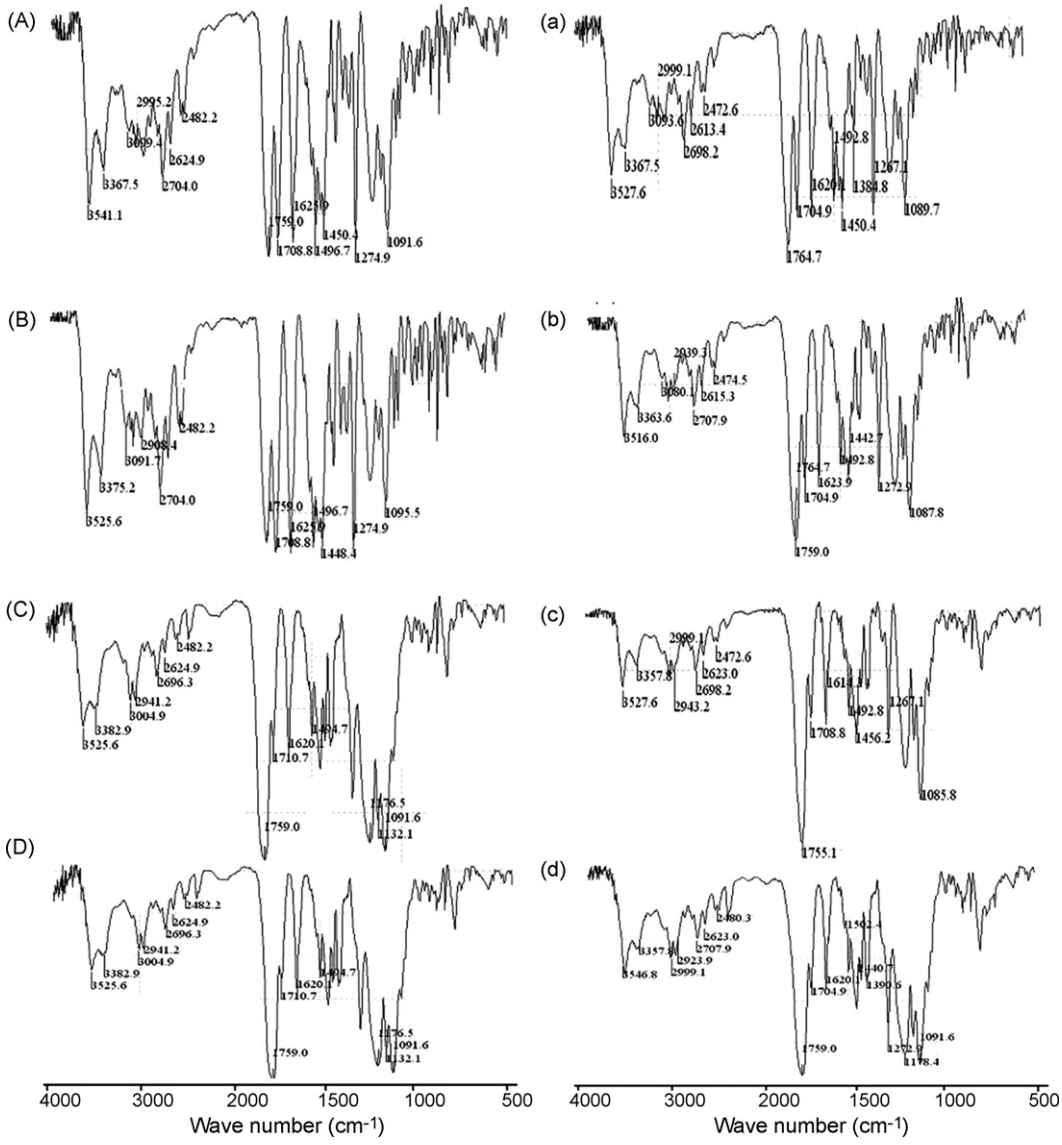

Fig. 12. The infrared spectra (IR) of ciprofloxacin-loaded PLGA microparticles with various drug/polymer ratios (w/w) (A) 1:1; (B) 1:2; (C) 1:3; (D) 1:5, and the respective physical mixtures (a) 1:1; (b) 1:2; (c) 1:3; (d) 1:5.

mal events, this relation was well determined. From DSC data, for the second DSC event occurred during the dehydration, it was observed a reduction of enthalpy values reached according to the drug content in the sample, which was confirmed by the intensity of the weight loss. The intensity of the thermal event in the range of 220–280 °C was related with the CP ratio present in the sample. Fig. 10 shows the correlation between the enthalpy values and the drug content for both, physical mixtures ($y = 4.41x - 270.58$; $r = 0.8811$) and drug-loaded PLGA microparticles ($3.12x - 193.77$; $r = 0.8656$). From the correlation coefficients (r) of the linear regression plot, it was demonstrated that this event occurred due to drug decomposition just a beginning of melting. Moreover, from T_g data it was possible to verify that the weight loss started just an initial melting of drug, indicating a thermal decomposition of the drug just a melting drug.

The same relationship was verified for the thermal event in the range of 280–330 °C, which was related to the polymer decomposition. It was possible to observe an increase of the enthalpy with the polymer ratio in the sample (Table 2).

The maintenance of the physicochemical properties of the pharmaceutical materials after the production process is fundamental for assuring the biological activity of the drug [24,26,42,43]. The DSC and TG/DTG analyses showed that thermal properties are very similar for both drug-loaded PLGA microparticles and respective physical mixtures, demonstrating that the stress conditions during spray drying process did not affect the thermal properties of the structural components of the microparticles.

The IR analysis was performed with an aim to complement the results obtained from thermal analysis. The IR spectra for both CP and PLGA are shown in Fig. 11.

The bands of the carboxyl OH group were assigned in the range of 2500–3500 cm^{-1}, the tertiary amine at 3527 and 3375 cm^{-1}, secondary amine at 3100, CH_2–N stretching at 2705 cm^{-1}, ketone C=O at 1708 cm^{-1}, C=C bands in the region of 1600 and 1495 cm^{-1} and C–F bond stretching in the range of 1100–1300 cm^{-1}, these values corresponding to the characteristic IR of CP (Fig. 11a). From the IR for PLGA (Fig. 11b) it was possible to identify the characteristic absorption bands at 1759 cm^{-1}, related to the ester group of PLGA, and axial stretching of sp2 and sp3 carbons in the range of 2900–3000 cm^{-1}, were assigned.

The IR spectra of the CP-loaded microparticles and the physical mixtures of the components are shown in Fig. 12.

For both, drug-loaded PLGA microparticles and different physical mixtures, the characteristic IR bands of the functional groups of CP and PLGA were established in a very similar fashion. On the contrary, the ester carbonyl groups of polymer could react with the amino groups of CP. However, the maintenance of the IR characteristic bands for both, drug and polymer, and the absence of the new IR bands, indicating modifications in the ester carbonyl and amine functions demonstrate that the drug is only dispersed in the PLGA polymeric matrix. Theses results are in agreement with the thermal analysis data indicating that they do not have significant interaction between the drug and the polymer used as structural component of the microparticles.

4. Conclusion

The results of this work demonstrated that through the thermal analysis it was possible to conduce the pre-formulation study for biodegradable microparticles produced by spray drying technique. The selected parameters for the microencapsulating process did not provoke any change in the physical and chemical stabilities of the microparticle components. It was possible to establish a relationship between the thermal behaviors of microparticles and the drug content. Thus, the technological parameters used to produce the microparticles provided a high degree of CP entrapment into polymeric matrix. Spray drying is an efficient and trustworthy technique for the production of CP-loaded microparticles.

Acknowledgements

The authors wish to thank FAPESP (A.G. Oliveira and T.P. Formariz), CNPq (A.G. Oliveira), CAPES (A.A. Silva-Junior) and PADC-FCF for the financial support. They also acknowledge the help of Timotty Roberts (MSc) in checking the English text.

References

[1] M.C. Callegan, M.C. Booth, M.S. Gilmore, Cornea 19 (2002) 539–545.
[2] I.S. Yalvac, N.E. Basci, A. Bozkurt, S. Duman, J. Cataract Refract. Surg. 29 (2003) 487–491.
[3] N.E. Basci, A. Bozkurt, D. Kalayci, S.O. Kayaalp, J. Pharm. Biomed. Anal. 14 (1996) 353–356.
[4] J.M. Anderson, M.S. Shive, Adv. Drug Deliv. Rev. 28 (1997) 5–24.
[5] E.K. Uhrich, M.S. Cannizzaro, S.R. Langer, M.K. Shakessheff, J. Am. Chem. Soc. 99 (1999) 3181–3198.
[6] R. Jain, N.H. Shah, A.W. Malick, C.T. Rhodes, Drug Dev. Ind. Pharm. 24 (1998) 703–727.
[7] A. Kunou, Y. Ogura, T. Yasukawa, H. Kimura, H. Miyamoto, Y. Honda, Y. Ykada, J. Control. Release 68 (2000) 263–271.
[8] T. Hickey, D. Kreutzer, D.J. Burgess, F. Moussy, Biomaterials 23 (2002) 1649–1656.
[9] R. Herrero-Vanrell, M.F. Refojo, Adv. Drug Deliv. Rev. 52 (2001) 5–16.
[10] M. Ramchandani, D. Robinson, J. Control. Release 54 (1998) 167–175.
[11] C. Désévaux, P. Dubreuil, V. Lenaerts, J. Control. Release 82 (2002) 83–93.
[12] K. Kanellakopoulou, M. Kolia, A. Anastasiadis, T. Korakis, E.J. Giamarellos-Bourboulis, A. Andreopoulos, E. Dounis, H. Giamarellou, Antimicrob. Agents Chemother. 43 (1999) 714–716.
[13] F. Damiana, N. Blatonb, P. Augustijnsa, L. Naesensc, J. Balzarinic, R. Kingeta, G. Van den Mootera, Thermochim. Acta 366 (2001) 61–69.
[14] S. Gaisford, G. Buckton, Thermochim. Acta 380 (2001) 185–198.
[15] J. Han, R. Suryanarayanan, Thermochim. Acta 329 (1999) 163–170.
[16] E. Rudnik, G. Matuschek, N. Milanov, A. Kettrup, Thermochim. Acta 427 (2005) 163–166.
[17] F.S. Souza, I.D. Basílio Jr., E.J. Oliveira, R.O. Macêdo, J. Therm. Anal. Calorim. 72 (2003) 549–554.
[18] A.C.D. Medeiros, L.P. Correia, M.O.S. Simões, R.O. Macêdo, J. Therm. Anal. Calorim. 88 (2007) 311–315.
[19] J.C. Jeong, J. Lee, K. Cho, J. Control. Release 92 (2003) 249–258.
[20] N.A. Rahman, E. Mathiowitz, J. Control. Release 94 (2004) 163–175.
[21] K. Feirong, J. Singh, Int. J. Pharm. 260 (2003) 149–156.
[22] C. Dubernet, Thermochim. Acta 248 (1995) 259–269.
[23] A.A. Silva-Júnior, Biodegradable microparticles for intraocular drug release, Master Thesis, Faculdade de Ciências Farmacêuticas de Araraquara-Unesp, Araraquara-SP, Brazil, 2005.

[24] A.A.S. Araújo, S. Storpirtis, L.P. Mercuri, F.M.S. Carvalho, M.S. Filho, J.R. Matos, Int. J. Pharm. 260 (2003) 303–314.
[25] D. Giron, J. Therm. Anal. Calorim. 68 (2002) 335–357.
[26] L.B. Lopes, M.V. Scarpa, N.L. Pereira, L.C. Oliveira, A.G. Oliveira, Braz. J. Pharm. Sci. 42 (2006) 497–504.
[27] A.A. Silva-Júnior, T.P. Formariz, M.V. Scarpa, A.G. Oliveira, J. Basic Appl. Pharm. Sci. 27 (2006) 119–126.
[28] E. Yonemochi, T. Hoshino, Y. Yoshihashi, K. Terad, Thermochim. Acta 432 (2005) 70–75.
[29] Y. Liu, J. Wang, Q. Yin, J. Crystal Growth 276 (2005) 237–242.
[30] I. Turel, P. Bukovec, Thermochim. Acta 287 (1996) 311–318.
[31] D. Bikiaris, G.Z. Papageorgiou, A. Stergiou, E. Pavlidou, E. Karavas, F. Kanaze, M. Georgarakis, Thermochim. Acta 439 (2005) 58–67.
[32] M.J. Arias, J.R. Moyano, J.M. Ginés, Thermochim. Acta 321 (1998) 33–41.
[33] Z. Naima, T. Siro, G.-D. Juan-Manuel, C. Chantal, C. René, D. Jerome, Eur. J. Pharm. Sci. 12 (2001) 395–404.
[34] K. Yamashita, T. Nakate, K. Okimoto, A. Ohike, Y. Tokunaga, R. Ibuki, K. Higaki, T. Kimura, Int. J. Pharm. 267 (2003) 79–91.
[35] O.I. Corrigan, Thermochim. Acta 248 (1995) 245–258.
[36] C. Gustafsson, T. Lennholm, C. Nystrom, Int. J. Pharm. 174 (1998) 243–252.
[37] A. Anshuman, K.R. Ambike, A.P. Mahadik, Int. J. Pharm. 282 (2004) 151–162.
[38] M. Ohta, G. Bucktona, Int. J. Pharm. 289 (2005) 31–38.
[39] S. Vyazovkin, I. Dranca, J. Phys. Chem. B 109 (2005) 18637–18644.
[40] S. Vyazovkin, I. Dranca, Pharm. Res. 23 (2006) 422–428.
[41] S.H. Kim, J.W. Chung, T.J. Kang, S.Y. Kwak, T. Suzuki, Polymer 48 (2007) 4271–4277.
[42] L. Mu, S.S. Feng, J. Control. Release 76 (2001) 239–254.
[43] Y.-J. Fu, S.-S. Shyu, F.-H. Su, P.-C. Yu, Colloids Surf. B: Biointerfaces 25 (2002) 269–279.